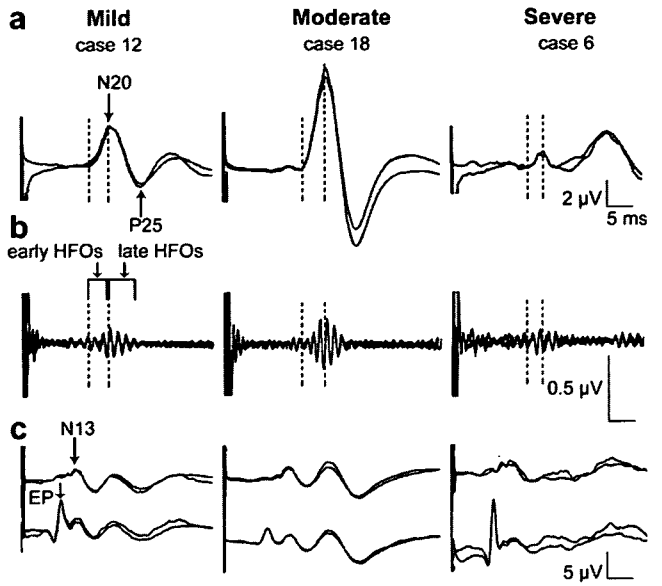

Fig. 1. Representative SEPs and HFOs in patients with different levels of weakness. Dotted line indicates the onset of N20. (a) N20 potential recorded from C3′ (C4′) to Fz montage. Note the amplitude of N20 markedly larger in the patient with moderate weakness (case 18) as compared with mild weakness patient (case 12). With severe weakness (case 6), a considerable decrease of the amplitude of N20 was observed. (b) HFOs obtained by digitally filtering raw SEPs from 500 to 1000 Hz. The amplitudes of early and late HFOs tend to be larger in a patient with moderate weakness than those with mild or severe weakness (c) Raw SEPs recorded from CV6-Fz and EP-Fz montage. Sufficient N9 and N13 potentials were evoked in all recordings.

For early HFOs (Fig. 3a, left), the group of subjects had a significant effect on their amplitude [$F(3,52) = 3.985$. $P = 0.013$]. The mean amplitudes were 0.15 ± 0.09 μV for healthy subjects, 0.19 ± 0.13 for mild, 0.28 ± 0.11 for moderate and 0.08 ± 0.05 for severe weakness groups. The amplitude of moderate weakness group was significantly larger than that of severe weakness group ($P = 0.013$). Although the difference was not significant ($P > 0.1$), the early HFOs changed in size in parallel with the size changes of main components of SEP in ALS. On the other hand, the amplitude of late HFOs (Fig. 3a, right) was not significantly affected by the group of subjects [$F(3,52) = 1.167$. $P = 0.331$] (control, 0.22 ± 0.14; mild, 0.23 ± 0.18; moderate 0.27 ± 0.12; severe, 0.11 ± 0.10). To evaluate relation between SEP main components and HFOs, the size ratios of oscillations to N20o–N20p amplitude are shown in Fig. 3b. There were no significant differences in these values among four groups ($P > 0.05$). This indicates that HFO amplitudes changed proportionally to the changes in main component amplitudes of SEP.

The numbers of HFO peaks at each part are listed in Table 2. There were no significant differences between healthy subjects and ALS patients ($P > 0.1$, unpaired Student's t-test). The group of subjects did not significantly affect the number of HFOs peaks at each part (onset–N20 peak; $F(3,52) = 1.760$, $P > 0.1$, later than N20 peak; $F(3,52) = 2.319$, $P > 0.05$).

3.2. SEP latencies

The latencies of P25p, N20o–N20p (duration of N20), and N13p–N20p (conventional CCT) of ALS patients (Table 2) were significantly longer than those of healthy subjects ($P < 0.05$, unpaired Student's t-test). The latencies of N13o, N20o, N13p, N20p, and N13o–N20o did not significantly differ between two groups. The group of subjects had a significant effect on P25p latency [$F(3,52) = 3.218$, $P = 0.032$]. The latency of mild weakness group was significantly longer than that of normal subjects ($P = 0.030$). The group of subjects did not affect the remaining latencies ($P > 0.05$).

3.3. CMAP amplitudes in APB

One way ANOVA revealed that the group of subjects had a significant effect on CMAP [$F(3,52) = 22.944$. $P < 0.001$]. The CMAP of control group was significantly larger than those of mild ($P < 0.001$), moderate ($P < 0.001$) and severe weakness groups ($P < 0.001$) (Table

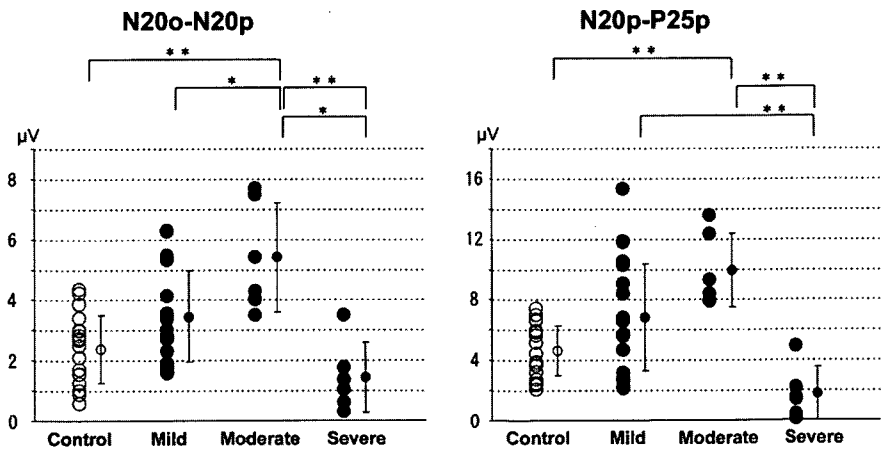

Fig. 2. Plots of the amplitudes of N20o–N20p (left) and N20p–P25p (right) components against the level of weakness. Circles indicate control subjects and dots ALS patients. Error bars indicate standard deviations. $^{*}P < 0.05$, $^{**}P < 0.01$.

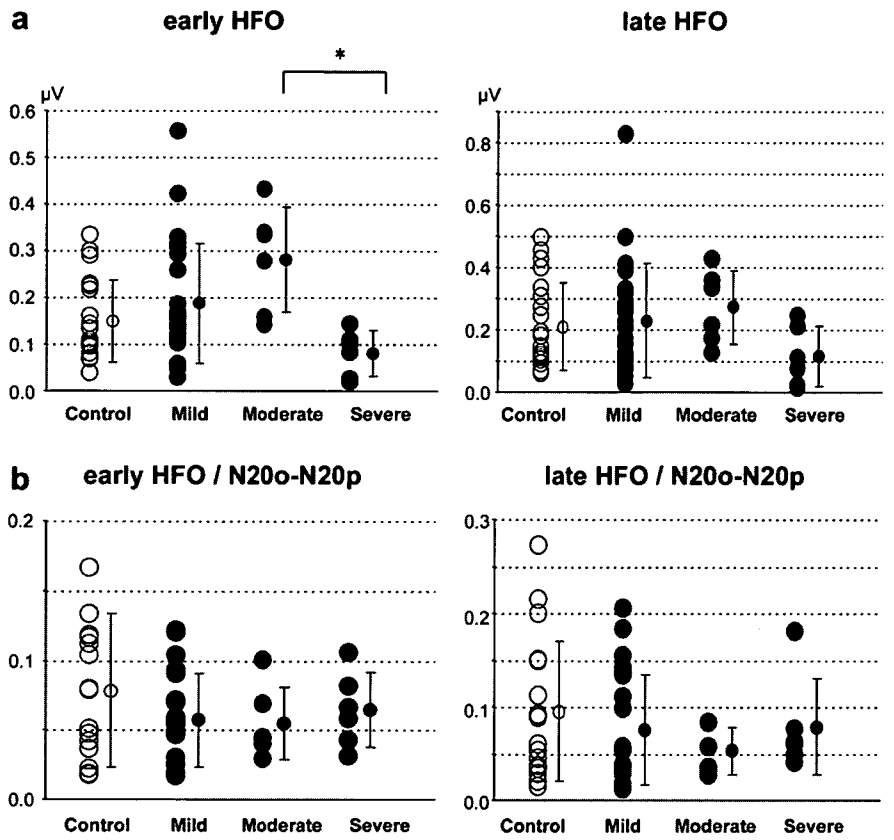

Fig. 3. (a) Plots of the amplitudes of early (left) and late (right) HFOs against the level of weakness. (b) Plots of the size ratio of HFOs to main component of SEP. $^{*}P < 0.05$.

2). There was also significant difference between mild and severe weakness groups ($P < 0.001$).

4. Discussion

We report three new findings. First, the amplitudes of N20o–N20p and N20p–P25p were abnormally enlarged in ALS patients with moderate weakness, while they attenuated in those with severe weakness. This was not due to insufficient peripheral stimulation because normal N9 potentials were elicited in all the patients. Second, both the early and late HFOs changed in size in parallel with the size changes of main components of SEP in ALS. The association between the main components and HFOs was confirmed by the constant size ratios of HFOs to the main component of SEP irrespective of the level of weakness. Finally, in ALS, the N13p–N20p conduction time (conventional CCT), N20o–N20p (duration of N20) and P25p latency were prolonged without any other latency abnormalities. Our present investigation is the first report about HFOs in ALS, and none of previous studies reported an enlargement of the N20 potential in ALS.

The N20 component of median nerve SEP is considered to reflect initial excitation of neurons in area 3b (Allison et al., 1991; Tiihonen et al., 1989). In contrast, even though several candidates have been proposed as a generator of HFOs, such as brainstem, thalamus, thalamocortical presynaptic action potentials and somatosensory cortex (Curio et al., 1997; Eisen et al., 1984; Gobbelé et al., 1998, 2004; Hashimoto et al., 1996, 1999; Klostermann et al., 2002; Shimazu et al., 2000), their generators remain to be determined (see a review by Mochizuki and Ugawa, 2005). The seminal work by Hashimoto et al. (1996) revealed the dissociation between SEP and HFOs amplitudes during a wake–sleep cycle. Thus, they proposed that HFOs reflect activities of inhibitory interneurons which are strongly associated with excitatory postsynaptic potentials (N20 amplitude) through feed forward and feed back inhibitions (Hashimoto et al., 1996; Nakano and Hashimoto, 1999; Tanosaki et al., 2002).

4.1. Amplitude changes in the N20 component

On the basis of the above notions, there are at least three possibilities to explain the SEP amplitude changes here reported in ALS.

(1) In humans, several studies using transcranial magnetic stimulation (TMS) indicate that pure sensory input can facilitate motor cortex (M1) (Hamdy et al., 1998; Kaelin-Lang et al., 2002; Ridding et al., 2000; Rosenkranz and Rothwell, 2003, 2004; Terao et al., 1995, 1999). These reports indicate there must be some mechanisms by which the sensory system mod-

ulates the motor cortical excitability. Corticocortical connections between areas 3a, 4 and 3b are present and topographically organized (Burton and Fabri, 1995; De Felipe et al., 1986; Krubitzer and Kaas, 1990). Thus, as well as subcortical structures, the sensory cortex might directly modulate the motor cortex. This sensory cortical driving of M1 may be enhanced to compensate for the affected motor cortex in ALS. This leads to the sensory cortical hyperexcitability, which is recognized as an enlargement of N20 potential in patients with moderate weakness. Then, small N20 in patients with severe weakness suggests that the compensation is no longer effective in those patients.

In ALS, the patients may need some mechanisms to compensate their weakness for precise and purposeful movements. One functional magnetic resonance imaging study suggested that cortical reorganization between motor related areas was a kind of partial compensation to optimize motor performances in ALS (Konrad et al., 2002). Some kind of compensatory function by non-motor system must exist in ALS patients. We speculate compensatory changes for motor dysfunction might occur not only in motor related areas but also in the somatosensory system. To use a weakened hand effectively, the patients may use sensory information much more powerfully than healthy subjects when they had moderate weakness, and these compensatory functions may disappear when the disease progresses because it becomes impossible to move their hands even with much compensation.

(2) The efferent signals from the motor cortex elicited by intracortical microstimulation diminished the size of any components of SEP generated by the sensory cortex in the monkey (Jiang et al., 1990). To date, various gating studies have confirmed that an early cortical response (N20) is attenuated by motor interferences (Gobbelé et al., 2003; Kakigi et al., 1995; Mochizuki et al., 2004; Rossini et al., 1999; Tanosaki et al., 2002; Valeriani et al., 1999). Though the precise mechanism is still a matter of controversy, one plausible explanation for this phenomenon is centrifugal gating hypothesis (Cohen and Starr, 1987). Attenuation of SEPs can be carried out by inhibitory interaction between the sensory signals and the efferent signals from motor related areas. Thus, in ALS patients, motor system disturbances may reduce inhibition of the sensory cortex, which finally leads to an enlargement of N20 potential. This possibility is unlike because SEPs were not enhanced but diminished in patients with severe weakness. If the above explanation is the case, SEPs would be more enhanced in the group of severe weakness.

Another possible influence on area 3b pyramidal cells by motor tasks is based on the intense cortico-cortical connections between area 3a and 3b (Kaas and Pons, 1988). Area 3a, which receives afferent signals from the muscles and joints, may reduce SEP sizes. This mechanism is called centripetal gating (Jones et al., 1989). We speculate the sensory input from muscle spindle must decrease in ALS because of inability of stretching spindles. This less gating of sensory cortex must enlarge the cortical potentials of SEP. This hypothesis also cannot explain the fact that SEPs were diminished in the patients with severe weakness.

(3) Neuropathological involvement of non-motor systems is well recognized in ALS patients. Neuronal loss may be seen in subcortical structures, including the basal ganglia, locus ceruleus, substantia nigra, thalamus, and so on (Lowe and Leigh, 2002). Based on the pathologically proven widespread involvement in ALS, one possible explanation for the N20/P25 changes is as follows: slight to moderate neuronal loss and gliosis were detected in the thalamic nuclei except for pulvinar thalamus in sporadic ALS patients who survived much longer with a respiratory support (Hayashi and Kato, 1989). It seems likely that some excitability changes occur in those thalamic nuclei in the late stage ALS. If the inhibitory reticular thalamic nucleus is involved, the N20 potential must be enhanced. If this is the case, SEPs must be enlarged even at the late stage of the ALS, which is inconsistent with our results.

Another possible explanation based on widespread involvement of extramotor systems is as follows. Some TMS studies revealed the lower motor threshold in the early stage of the ALS (Eisen et al., 1993; Mills and Nithi, 1997), and the others revealed abnormal firing patterns in the peristimulus time histograms in ALS (Eisen et al., 1996; Kohara et al., 1996; Mills, 1995). These results suggested the corticomotor hyperexcitability. This hyperexcitability is considered to be due to monoamine neuroexcitotoxicity in ALS. Therefore, we can speculate that similar neuroexcitotoxic changes occur in the sensory cortex, one of extramotor systems, which must cause SEP enlargements. Further studies are needed to determine whether it is the case in ALS.

4.2. Amplitude changes in the HFOs

The results showed that the early and late HFOs tended to be enlarged in patients with moderate weakness. The HFO/N20 amplitude ratios were not affected by the degree of weakness.

According to the hypothesis proposed by Hashimoto and coworkers, HFOs must reflect activities of inhibitory interneurons activated by both thalamocortical afferents and excitatory synaptic inputs from pyramidal neurons of area 3b through their local axon collaterals (Hashimoto et al., 1996; Nakano and Hashimoto, 1999; Tanosaki et al., 2002). If so, they reflect both feed forward and feed

back inhibitory effects onto the post synaptic pyramidal neurons of the sensory cortex. They claimed that one function of inhibitory interneurons of the sensory cortex must be a stabilization of the pyramidal cell activity, similar to that of Renshow cell in the spinal cord (Tanosaki et al., 2002). Based on this hypothesis, we can speculate that, in ALS patients with moderate weakness, the compensatory hyperexcitable sensory cortex may be stabilized by inhibitory interneurons comparably active to the hyperexcitable pyramidal neurons. In patients with severe weakness, inhibitory interneurons may not be activated because of the low activity of excitatory sensory pyramidal neurons. Such modulation from the pyramidal neurons toward the interneurons can explain the parallel behavior of HFO and N20/P25 potential and also explain some previous results which show the absence of a dissociation between HFOs and main components of SEP in aged or young healthy subjects and in patients with myoclonus epilepsy (Mochizuki et al., 1999; Nakano and Hashimoto, 1999, 2000). Another possibility to explain our results is that HFOs do not purely reflect the inhibitory interneuron activities and the dissociation between HFOs and SEP components is not a universal phenomenon.

4.3. Sensory conduction time in ALS

Many studies of SEP in ALS are conflicting: some reports revealed no SEP abnormalities (Cascino et al., 1988; Chiappa, 1983; Oh et al., 1985), while others showed conduction delays in upper limb SEPs (Bosch et al., 1985; Cosi et al., 1984; Dasheiff et al., 1985; Radtke et al., 1986; Subramaniam and Yiannikas, 1990; Theys et al., 1999; Zanette et al., 1990) and lower limb SEPs (Georgesco et al., 1997; Matheson et al., 1986; Radtke et al., 1986; Subramaniam and Yiannikas, 1990; Zanette et al., 1996). They were delays of N13–N19 (Bosch et al., 1985; Cosi et al., 1984; Subramaniam and Yiannikas, 1990; Zanette et al., 1990) and N9–N20 interpeak latencies (Radtke et al., 1986; Theys et al., 1999). The prolonged conventional CCT in our results is consistent with such previous studies. However, we should interpret these results carefully. The interpeak latency of N13–N20 is widely accepted as "central sensory conduction time" even though various issues concerning them remain to be investigated (Sonoo et al., 1996; Tanosaki et al., 1999). Because the amplitude of N20 positively correlated with its duration (Sonoo et al., 1997), alternation of the N20 amplitude may cause changes in the conventional CCT. In ALS, the enhanced N20 must cause prolongation of the conventional CCT and duration of N20. In addition, no differences were found in any other latency parameters between ALS and healthy subjects; the onset latency of N13 and N20, the interval of N13o–N20o and the peak latency of N13 and N20. These suggest that the intracranial sensory conduction was not prolonged in ALS. Based on these, we conclude that in ALS, the prolonged conventional CCT is not due to a conduction delay in the central sensory system but due to a prolongation of N20 production processes.

Based on the above arguments, we have two conclusions. (1) The amplitude alternation of N20 potential has some relation with the severity of weakness. Enlarged N20 potential must reflect somatosensory compensation for motor system dysfunction in ALS. (2) In ALS patients, the prolonged conventional CCT does not indicate a conduction delay in the sensory system, but it suggests an alternation of some central sensory processing.

Acknowledgements

Part of this work was supported by Research Project Grant-in-aid for Scientific Research No. 17590865 (RH), No. 18590928 (YT), No. 16500194 (YU) from the Ministry of Education, Science, Sports and Culture of Japan, grants for the Research Committee on rTMS treatment of movement disorders, the Ministry of Health and Welfare of Japan (17231401), the Research Committee on dystonia, the Ministry of Health and Welfare of Japan, a grant from the Committee of the Study of Human Exposure to EMF, Ministry of Public Management, Home Affairs, Post and Telecommunications.

References

Allison T, McCarthy G, Wood CC, Jones SJ. Potentials evoked in human and monkey cerebral cortex by stimulation of the median nerve. A review of scalp and intracranial recordings. Brain 1991;114:2465–503.

Bosch EP, Yamada T, Kimura J. Somatosensory evoked potentials in motor neuron disease. Muscle Nerve 1985;8:556–62.

Brooks BR, Miller RG, Swash M, Munsat TL. World Federation of Neurology Research Group on Motor Neuron Diseases. El Escorial revisited: revised criteria for the diagnosis of amyotrophic lateral sclerosis. Amyotroph Lateral Scler Other Motor Neuron Disord 2000;1:293–9.

Burton H, Fabri M. Ipsilateral intracortical connections of physiologically defined cutaneous representations in areas 3b and 1 of macaque monkeys: projections in the vicinity of the central sulcus. J Comp Neurol 1995;355:508–38.

Cascino GD, Ring SR, King PJ, Brown RH, Chiappa KH. Evoked potentials in motor system diseases. Neurology 1988;38:231–8.

Chiappa KH. Evoked potentials in clinical medicine. New York: Raven Press; 1983.

Cohen LG, Starr A. Localization, timing and specificity of gating of somatosensory evoked potentials during active movement in man. Brain 1987;110:451–67.

Cosi V, Poloni M, Mazzini L, Callieco R. Somatosensory evoked potentials in amyotrophic lateral sclerosis. J Neurol Neurosurg Psychiatry 1984;47:857–61.

Curio G, Marckert BM, Burghoff M, Koetitz R, Abraham-Fuchs K, Härer W. Localization of evoked neuromagnetic 600 Hz activity in the cerebral somatosensory system. Electroenceph Clin Neurophysiol 1994;91:483–7.

Curio G, Mackert BM, Burghoff M, Neumann J, Nolte G, Scherg M, et al. Somatotopic source arrangement of 600 Hz oscillatory magnetic fields at the human primary somatosensory hand cortex. Neurosci Lett 1997;234:131–4.

Dasheiff RM, Drake ME, Brendle A, Erwin CW. Abnormal somatosensory evoked potentials in amyotrophic lateral sclerosis. Electroenceph Clin Neurophysiol 1985;60:306–11.

de Carvalho M, Swash M. Nerve conduction studies in amyotrophic lateral sclerosis. Muscle Nerve 2000;23:344–52.

De Felipe J, Conley M, Jones EG. Long-range focal collateralization of axons arising from corticocortical cells in monkey sensory-motor cortex. J Neurosci 1986;6:3749–66.

Eisen A, Roberts K, Low M, Hoirch M, Lawrence P. Questions regarding the sequential neural generator theory of the somatosensory evoked potential raised by digital filtering. Electroenceph Clin Neurophysiol 1984;59:388–95.

Eisen A, Pant B, Stewart H. Cortical excitability in amyotrophic lateral sclerosis: a clue to pathogenesis. Can J Neurol Sci 1993;20:11–6.

Eisen A, Entezari Taher M, Stewart H. Cortical projections to spinal motoneurons: changes with aging and amyotrophic lateral sclerosis. Neurology 1996;46:1396–404.

Emerson RG, Sgro JA, Pedley TA, Hauser WA. State-dependent changes in the N20 component of the median nerve somatosensory evoked potential. Neurology 1988;38:64–8.

Georgesco M, Salerno A, Camu W. Somatosensory evoked potentials elicited by stimulation of lower-limb nerves in amyotrophic lateral sclerosis. Electroenceph Clin Neurophysiol 1997;104: 333–42.

Gobbelé R, Buchner H, Curio G. High-frequency (600 Hz) SEP activities originating in the subcortical and cortical human somatosensory system. Electroencephalogr Clin Neurophysiol 1998;108: 182–9.

Gobbelé R, Waberski TD, Kuelkens S, Sturm W, Curio G, Buchner H. Thalamic and cortical high-frequency (600 Hz) somatosensory-evoked potential (SEP) components are modulated by slight arousal changes in awake subjects. Exp Brain Res 2000;133:506–13.

Gobbelé R, Waberski TD, Thyerlei D, Thissen M, Darvas F, Klostermann F, et al. Functional dissociation of a subcortical and cortical component of high-frequency oscillations in human somatosensory evoked potentials by motor interference. Neurosci Lett 2003;350:97–100.

Gobbelé R, Waberski TD, Simon H, Peters E, Klostermann F, Curio G, et al. Different origins of low and high frequency components (600 Hz) of human somatosensory evoked potentials. Clin Neurophysiol 2004;115:927–37.

Hamdy S, Rothwell JC, Aziz Q, Singh KD, Thompson DG. Long-term reorganization of human motor cortex driven by short-term sensory stimulation. Nat Neurosci 1998;1:64–8.

Hashimoto I, Mashiko T, Imada T. Somatic evoked high-frequency magnetic oscillations reflect activity of inhibitory interneurons in the human somatosensory cortex. Electroenceph Clin Neurophysiol 1996;100:189–203.

Hashimoto I, Kimura T, Fukushima T, Iguchi Y, Saito Y, Terasaki O, et al. Reciprocal modulation of somatosensory evoked N20m primary response and high-frequency oscillations by interference stimulation. Clin Neurophysiol 1999;110:1445–51.

Haueisen J, Heuer T, Nowak H, Liepert J, Weiller C, Okada Y, et al. The influence of lorazepam on somatosensory-evoked fast frequency (600 Hz) activity in MEG. Brain Res 2000;874:10–4.

Hayashi H, Kato S. Total manifestations of amyotrophic lateral sclerosis. ALS in the totally locked-in state. J Neurol Sci 1989;93:19–35.

Inoue K, Hashimoto I, Shirai T, Kawakami H, Miyachi T, Mimori Y, et al. Disinhibition of the somatosensory cortex in cervical dystonia – decreased amplitudes of high frequency oscillations. Clin Neurophysiol 2004;115:1624–30.

Jiang W, Chapman CE, Lamarre Y. Modulation of somatosensory evoked responses in the primary somatosensory cortex produced by intracortical microstimulation of the motor cortex in the monkey. Exp Brain Res 1990;80:333–44.

Jones SJ, Halonen JP, Shawkat F. Centrifugal and centripetal mechanisms involved in the 'gating' of cortical SEPs during movement. Electroenceph Clin Neurophysiol 1989;74:36–45.

Kaas JH, Pons TP. The somatosensory system in primates. Comp Primate Biol 1988;4:421–68.

Kaelin-Lang A, Luft AR, Sawaki L, Burstein AH, Sohn YH, Cohen LG. Modulation of human corticomotor excitability by somatosensory input. J Physiol 2002;540:623–33.

Kakigi R, Koyama S, Hoshiyama M, Watanabe S, Shimojo M, Kitamura Y. Gating of somatosensory evoked responses during active finger movements magnetoencephalographic studies. J Neurol Sci 1995;128:195–204.

Kimura J. Electrodiagnosis in diseases of nerve and muscle: principles and practice. 3rd ed. New York, NY: Oxford University Press; 2001.

Klostermann F, Nolte G, Curio G. Multiple generators of 600 Hz wavelets in human SEP unmasked by varying stimulus rates. Neuroreport 1999;10:1625–9.

Klostermann F, Funk T, Vesper J, Siedenberg R, Curio G. Double-pulse stimulation dissociates intrathalamic and cortical high-frequency (>400 Hz) SEP components in man. Neuroreport 2000;11:1295–9.

Klostermann F, Gobbelé R, Buchner H, Curio G. Intrathalamic non-propagating generators of high-frequency (1000 Hz) somatosensory evoked potential (SEP) bursts recorded subcortically in man. Clin Neurophysiol 2002;113:1001–5.

Kohara N, Kaji R, Kojima Y, Mills KR, Fujii H, Hamano T, et al. Abnormal excitability of the corticospinal pathway in patients with amyotrophic lateral sclerosis: a single motor unit study using transcranial magnetic stimulation. Electroenceph Clin Neurophsiol 1996;101:32–41.

Konrad C, Henningsen H, Bremer J, Mock B, Deppe M, Buchinger C, et al. Pattern of cortical reorganization in amyotrophic lateral sclerosis: a functional magnetic resonance imaging study. Exp Brain Res 2002;143:51–6.

Krubitzer LA, Kaas JH. The organization and connections of somatosensory cortex in marmosets. J Neurosci 1990;10:952–74.

Lowe JS, Leigh N. Disorders of movement and system degenerations. In: Graham DI, Lantos PL, editors. Greenfield's neuropathology. 7th ed. New York, NY: Oxford University Press; 2002. p. 372–83.

Matheson JK, Harrington HJ, Hallett M. Abnormalities of multimodality evoked potentials in amyotrophic lateral sclerosis. Arch Neurol 1986;43:338–40.

Mills KR. Motor neuron disease. Studies of the corticospinal excitation of single motor neurons by magnetic brain stimulation. Brain 1995;118:971–82.

Mills KR, Nithi K. Corticomotor threshold is reduced in early idiopathic amyotrophic lateral sclerosis. Muscle Nerve 1997;20:1137–41.

Mochizuki H, Ugawa Y. High-frequency oscillations in somatosensory system. Clin EEG Neurosci 2005;36:278–84.

Mochizuki H, Ugawa Y, Machii K, Terao Y, Hanajima R, Furubayashi T, et al. Somatosensory evoked high-frequency oscillation in Parkinson's disease and myoclonus epilepsy. Clin Neurophysiol 1999;110:185–91.

Mochizuki H, Terao Y, Okabe S, Furubayashi T, Arai N, Iwata NK, et al. Effects of motor cortical stimulation on the excitability of contralateral motor and sensory cortices. Exp Brain Res 2004;158:519–26.

Nakano S, Hashimoto I. The later part of high-frequency oscillations in human somatosensory evoked potentials is enhanced in aged subjects. Neurosci Lett 1999;276:83–6.

Nakano S, Hashimoto I. High-frequency oscillations in human somatosensory evoked potentials are enhanced in school children. Neurosci Lett 2000;291:113–6.

Oh SJ, Sunwoo IN, Kim HS, Faught E. Cervical and cortical somatosensory evoked potentials differentiate cervical spondylotic myelopathy from amyotrophic lateral sclerosis (abstract). Neurology 1985;35 suppl 1:147–8.

Radtke RA, Erwin A, Erwin CW. Abnormal sensory evoked potentials in amyotrophic lateral sclerosis. Neurology 1986;36:796–801.

Ridding MC, Brouwer B, Miles TS, Pitcher JB, Thompson PD. Changes in muscle responses to stimulation of the motor cortex induced by peripheral nerve stimulation in human subjects. Exp Brain Res 2000;131:135–43.

Rosenkranz K, Rothwell JC. Differential effect of muscle vibration on intracortical inhibitory circuits in humans. J Physiol 2003;551: 649–60.

Rosenkranz K, Rothwell JC. The effect of sensory input and attention on the sensorimotor organization of the hand area of the human motor cortex. J Physiol 2004;561:307–20.

Rossini PM, Babiloni C, Babiloni F, Ambrosini A, Onorati P, Carducci F, et al. "Gating" of human short-latency somatosensory evoked cortical responses during execution of movement. A high resolution electroencephalography study. Brain Res 1999;843:161–70.

Shimazu H, Kaji R, Tsujimoto T, Kohara N, Ikeda A, Kimura J, et al. High-frequency SEP components generated in the somatosensory cortex of the monkey. Neuroreport 2000;11:2821–6.

Sonoo M, Kobayashi M, Genba-Shimizu K, Mannen T, Shimizu T. Detailed analysis of the latencies of median nerve somatosensory evoked potential components, 1: selection of the best standard parameters and the establishment of normal values. Electroenceph Clin Neurophysiol 1996;100:319–31.

Sonoo M, Genba-Shimizu K, Mannen T, Shimizu T. Detailed analysis of the latencies of median nerve somatosensory evoked potential components, 2: analysis of subcomponents of the P13/14 and N20 potentials. Electroenceph Clin Neurophysiol 1997;104:296–311.

Subramaniam JS, Yiannikas C. Multimodality evoked potentials in motor neuron disease. Arch Neurol 1990;47:989–94.

Tanosaki M, Ozaki I, Shimamura H, Baba M, Matsunaga M. Effects of aging on central conduction in somatosensory evoked potentials: evaluation of onset versus peak methods. Clin Neurophysiol 1999;110:2094–103.

Tanosaki M, Kimura T, Takino R, Iguchi Y, Suzuki A, Kurobe Y, et al. Movement interference attenuates somatosensory high-frequency oscillations: contribution of local axon collaterals of 3b pyramidal neurons. Clin Neurophysiol 2002;113:993–1000.

Terao Y, Ugawa Y, Uesaka Y, Hanajima R, Gemba-Shimizu K, Ohki Y, et al. Input–output organization in the hand area of the human motor cortex. Electroenceph Clin Neurophysiol 1995;97:375–81.

Terao Y, Ugawa Y, Hanajima R, Furubayashi T, Machii K, Enomoto H, et al. Air-puff-induced facilitation of motor cortical excitability studied in patients with discrete brain lesions. Brain 1999;122:2259–77.

Theys PA, Peeters E, Robberecht W. Evolution of motor and sensory deficits in amyotrophic lateral sclerosis estimated by neurophysiological techniques. J Neurol 1999;246:438–42.

Tiihonen J, Hari R, Hämäläinen M. Early deflections of cerebral magnetic responses to median nerve stimulation. Electroenceph Clin Neurophysiol 1989;74:290–6.

Valeriani M, Restuccia D, Di Lazzaro V, Le Pera D, Tonali P. Effect of movement on dipolar source activities of somatosensory evoked potentials. Muscle Nerve 1999;22:1510–9.

Yamada T, Kameyama S, Fuchigami Y, Nakazumi Y, Dickins QS, Kimura J. Changes of short latency somatosensory evoked potential in sleep. Electroenceph Clin Neurophysiol 1988;70:126–36.

Zanette G, Polo A, Gasperini M, Bertolasi L, de Grandis D. Far-field and cortical somatosensory evoked potentials in motor neuron disease. Muscle Nerve 1990;13:47–55.

Zanette G, Tinazzi M, Polo A, Rizzuto N. Motor neuron disease with pyramidal tract dysfunction involves the cortical generators of the early somatosensory evoked potential to tibial nerve stimulation. Neurology 1996;47:932–8.

J Neurosurg 107:548–554, 2007

Characteristics and distribution of somatosensory evoked potentials in the subthalamic region

MAYUMI KITAGAWA, M.D., PH.D.,[1] JUN-ICHI MURATA, M.D., PH.D.,[2] HARUO UESUGI, M.D., PH.D.,[1] RITSUKO HANAJIMA, M.D., PH.D.,[3] YOSHIKAZU UGAWA, M.D., PH.D.,[4] AND HISATOSHI SAITO, M.D.[2]

Departments of [1]Neurology and [2]Neurosurgery, Sapporo Azabu Neurosurgical Hospital, Sapporo; [3]Department of Neurology, Tokyo University of Medicine, Tokyo; and [4]Department of Neurology, School of Medicine, Fukushima Medical University, Fukushima, Japan

Object. The aim of the present study is to evaluate the topographical distribution of somatosensory evoked potentials (SSEPs) in the subthalamic area, including the zona incerta (ZI). Determination of this distribution may help in the correct placement of deep brain stimulation (DBS) leads.

Methods. Intraoperative SSEPs were recorded from contacts of DBS electrodes at 221 sites in 41 patients: three patients with essential tremor and 38 with Parkinson disease who underwent implantation of DBS electrodes for the relief of severe tremor or parkinsonism.

Results. Two distinct SSEPs were recorded in the subthalamic area. One was a monophasic positive wave with a mean latency of 15.8 ± 0.9 msec, which the authors designated subthalamic P16. Using both cephalic and noncephalic references, subthalamic P16 was only recorded in the ventral part of the ZI (mean 6.6 ± 1. 3 mm posterior to the midcommissure point, 4.8 ± 1.2 mm inferior to the anterior commissure–posterior commissure line, and 9.7 ± 0.6 mm lateral to the midline). When bipolar recordings were made, the traces showed a phase reversal at the caudal part of the ZI. The second potential is a positive–negative SSEP recorded throughout the entire subthalamic area. The mean latencies of the initial positive peak and the major negative peak were 13.6 ± 1.1 msec and 16.4 ± 1.1 msec, respectively. Several small notches were superimposed on the peaks, and their amplitudes were largest at the contact close to the medial lemniscus.

Conclusions. The results indicate that intraoperative SSEPs from DBS electrodes are helpful in refining stereotactic targets in the thalamus and subthalamic areas. *(DOI: 10.3171/JNS-07/09/0548)*

KEY WORDS • **deep brain stimulation** • **somatosensory evoked potential** • **stereotactic target** • **subthalamus** • **zona incerta**

OVER the past decade, DBS has been used in the treatment of various movement disorders. Stimulation of the Vim has generally been used to treat severe tremor,[2] and stimulation of the dorsolateral STN and adjacent subthalamic area can improve all levodopa-responsive symptoms in patients with PD.[15,19] Recently some groups, including our own, have reported that stimulation of the posterior subthalamic region, which includes the ZI and the prelemniscal radiation, can improve not only severe tremor but also rigidity and akinesia in patients with PD.[7,11,14,18]

Both radiological and electrophysiological studies are important in the determination of optimal target positions for stereotactic surgery. Microelectrode recording of spontaneous neuronal activities is used to ensure optimal placement for treatment. However, when the target is located in white matter areas such as the posterior subthalamic region, it is difficult to determine the target position by relying on recordings of spontaneous neuronal activities. In addition to spontaneous neuronal activities, SSEPs are also used for localizing the electrodes in the thalamus, ML, prelemniscal radiation, and STN.[5,6,8,9,16] Using a quadripolar implanted DBS electrode, SSEPs can be recorded simultaneously from these four different sites 3 mm apart. We recently reported that SSEPs recorded in the presumed site of the ZI demonstrated a prominent positive component with fine notches.[7,11] The aim of the present study is to evaluate the topographical distribution of SSEPs in the posterior subthalamic area (including the ZI), which may aid in the correct placement of the DBS lead.

Abbreviations used in this paper: AC = anterior commissure; CT = computed tomography; DBS = deep brain stimulation; ML = medial lemniscus; MR = magnetic resonance; PC = posterior commissure; PD = Parkinson disease; SSEP = somatosensory evoked potential; STN = subthalamic nucleus; Vc = nucleus ventrocaudalis; Vim = nucleus ventralis intermedius; ZI = zona incerta.

Clinical Material and Methods

Patient Population

We analyzed 221 SSEPs recorded in 41 patients (three patients with essential tremor and 38 with PD) in whom

DBS electrodes were implanted (Table 1). Electrodes were implanted in the region of the ZI and prelemniscal radiation in three patients with essential tremor and in 16 patients who had PD and a severe resting tremor rated at least 3/4 according to Item 20 of the Unified PD Rating Scale. Electrodes were implanted at the STN in 22 patients with advanced PD and severe motor function fluctuations. Informed consent was obtained from all patients.

TABLE 1

*Patient clinical characteristics and targets of electrode implantation**

Case No.	Age (yrs), Sex	Disease	Target Region (side)
1	63, F	PD	ZI/Prl (rt)
2	65, M	PD	ZI/Prl (rt)
3	67, M	PD	ZI/Prl (lt)
4	40, M	PD	ZI/Prl (lt)
5	67, F	PD	ZI/Prl (lt)
6	44, M	PD	ZI/Prl (lt)
7	67, M	PD	ZI/Prl (lt)
8	76, M	PD	ZI/Prl (lt)
9	56, M	PD	ZI/Prl (lt)
10	54, M	PD	ZI/Prl (lt)
11	49, F	PD	ZI/Prl (lt)
12	69, M	PD	ZI/Prl (lt)
13	65, M	PD	ZI/Prl (lt)
14	64, M	PD	ZI/Prl (both)
15	67, M	PD	ZI/Prl (both)
16	74, F	ET	ZI/Prl (rt)
17	57, M	ET	ZI/Prl (lt)
18	63, M	ET	ZI/Prl (lt)
19	72, M	PD	ZI/Prl (rt), STN (lt)
20	68, F	PD	STN (rt)
21	63, M	PD	STN (rt)
22	67, F	PD	STN (rt)
23	63, M	PD	STN (rt)
24	62, M	PD	STN (rt)
25	53, M	PD	STN (rt)
26	58, M	PD	STN (lt)
27	68, M	PD	STN (lt)
28	80, F	PD	STN (lt)
29	67, M	PD	STN (lt)
30	67, F	PD	STN (lt)
31	63, F	PD	STN (both)
32	63, M	PD	STN (both)
33	76, F	PD	STN (both)
34	68, M	PD	STN (both)
35	63, F	PD	STN (both)
36	70, M	PD	STN (both)
37	72, M	PD	STN (both)
38	46, M	PD	STN (both)
39	54, M	PD	STN (both)
40	64, F	PD	STN (both)
41	59, F	PD	STN (both)

* ET = essential tremor; Prl = prelemniscal radiation.

Surgical Procedures

The surgical methods used were essentially the same as those previously reported by our group.[7,11] Axial T2-weighted MR images (Signa Excite 1.5-tesla, General Electric; TR 4000 msec, TE 92.3 msec) were obtained in 2-mm slice thickness without interslice spacing on the day before surgery. The STN, red nucleus, AC, and PC were clearly identified on the high-resolution images. On the day of surgery, after a Cosman-Roberts-Wells frame (Radionics Inc.) had been attached to the patient's skull, CT scans of 1-mm slice thickness were obtained. The MR and CT images were fused with the aid of ImageFusion (Radionics) so that a high quality of anatomical resolution could be maintained without spatial distortion. Tentative targets in either the subthalamic white matter or the STN were initially determined on the axial MR–CT fused images. The anatomical location of each target was confirmed using AtlasPlan software (Radionics), in which images from the Schaltenbrand–Wahren atlas are superimposed onto MR–CT fused images with registration of the AC and PC as references. The tentative target for the ZI–prelemniscal radiation region was located at a point just lateral to the most lateral border of the red nucleus (~ 10 mm lateral to the midline), and 3 to 4 mm posterior to the posterior border of the STN on the axial slice in which the STN appeared largest. A trajectory was planned to pass through the Vim–ventrooralis posterior nuclei at an angle of approximately 60° from the AC–PC line. The procedure used to determine the STN target was similar to that reported in recent articles citing the MR imaging–based direct targeting method,[1] and the trajectory was planned to pass through the center of the STN at an angle approximately 50° from the AC–PC line.

Electrophysiological Recording

Intraoperative macrostimulation was used to confirm therapeutic effects and check adverse responses at each target location. The probe was then replaced with a quadripolar DBS electrode (model 3387; Medtronic, Inc.) that had four contacts numbered 0, 1, 2, and 3 from the tip of the electrode. The contacts were 1.5 mm long and spaced 1.5 mm apart. Four extension cords from each contact were connected to different input ports on the evoked potential recorder (Synax, model ER2100; NEC). The Ag/AgCl surface cup electrodes were placed at several points, including the NC (noncephalic reference on the contralateral shoulder), Fz (midline frontal), and CPc (centroparietal). The contralateral median nerve was stimulated at the wrist by applying 5-Hz electric square wave pulses, 0.2 msec in duration, 1.1 to 1.2 times the motor threshold in intensity. Two hundred fifty single responses were averaged using a bandpass filter setting between 2 and 2500 Hz. Recordings were made from the four contacts of the DBS electrode with monopolar noncephalic (0-NC, 1-NC, 2-NC, 3-NC), monopolar cephalic (0-Fz, 1-Fz, 2-Fz, 3-Fz), and bipolar (0-1, 1-2, 2-3) configurations. After the electrode had been firmly affixed to the skull, the SSEPs were recorded again. The averaged responses were stored on data disks of the evoked potential recorder for later offline analysis. The peak latency and amplitude of major components of the SSEPs were measured on the recording provided by the fixed leads.

Electrode Localization

Immediately postoperatively, axial MR images were obtained with the same MR parameters. Using ImageFusion, postoperative MR images were fused with preoperative stereotactic CT scans to make the preoperative coordinate system available for the postoperative images. The deepest contact (Contact 0) was identified on the axial and

sagittal reconstruction images, with careful avoidance of the metallic artifacts that appeared just a few millimeters below the deepest contact. The coordinates of Contact 0 were calculated using the targeting software (StereoPlan, Radionics). The coordinates of the upper contacts (Contacts 1–3) were calculated by retracting the target along the trajectory by 3, 6, and 9 mm, respectively.

Results

Figure 1 shows an example of simultaneous SSEPs from the scalp and four contacts (0, 1, 2, and 3) of the DBS electrode along the trajectory to the ZI and the prelemniscal radiation. The scalp P9, P13/14, and N18 were well identified in the Cpc-NC and Fz-NC lead. The mean latencies of P13/14 and the initial negative peak of N18 were 13.6 ± 1.1 msec and 16.3 ± 1.1 msec, respectively. The scalp N20 was well identified in the Cpc-Fz lead, and the mean latency of N20 was 19.5 ± 1.1 msec.

Subthalamic Region SSEPs with Cephalic and Noncephalic References

Figure 2 shows examples of SSEPs from the DBS electrode along the trajectory to the ZI and prelemniscal radiation (Fig. 2A) and those to the STN (Fig. 2B). Using cephalic (Fz) and noncephalic references, two distinct SSEPs were recorded in the subthalamic area. One was a positive–negative wave recorded in various subthalamic areas including the prelemniscal radiation, ML, and STN. The other was a monophasic positive wave recorded only in the posteromedial subthalamic region. Figure 3 shows the distribution of SSEPs with identical configurations in the Schaltenbrand–Wahren atlas.

Positive–Negative Wave

Positive–negative waves were recorded in the various subthalamic areas including the prelemniscal radiation (2-Fz and 3-Fz, Fig. 1; 3-Fz and 3-NC, Fig. 2A), ML (0-Fz and 0-NC, Fig. 2A) and STN (0-Fz and 1-Fz, Fig. 2B). The peak latencies of the positive–negative SSEPs were almost the same as those of the scalp CPc-NC and Fz-NC SSEPs (Fig. 1). The mean latency of the positive peak of the biphasic wave was 13.6 ± 1.1 msec (209 SSEPs), which was the same as that of scalp P13/14. The mean latency of the negative peak was 16.4 ± 1.1 msec, which was almost the same as that of N18. The mean amplitudes of the positive and negative peaks in relation to the sites of recording are summarized in Fig. 4. The amplitude of the initial positive peak was maximal in the ventral part of the ZI (6.0 ± 4.3 μV, 27 SSEPs), while the amplitude of the negative peak was maximal in the STN (6.9 ± 2.0 μV, 58 SSEPs).

Several small notches were distributed between initial positive and major negative peaks. The small notches became large when the contact was located close to the ML (Figs. 1 and 2A).

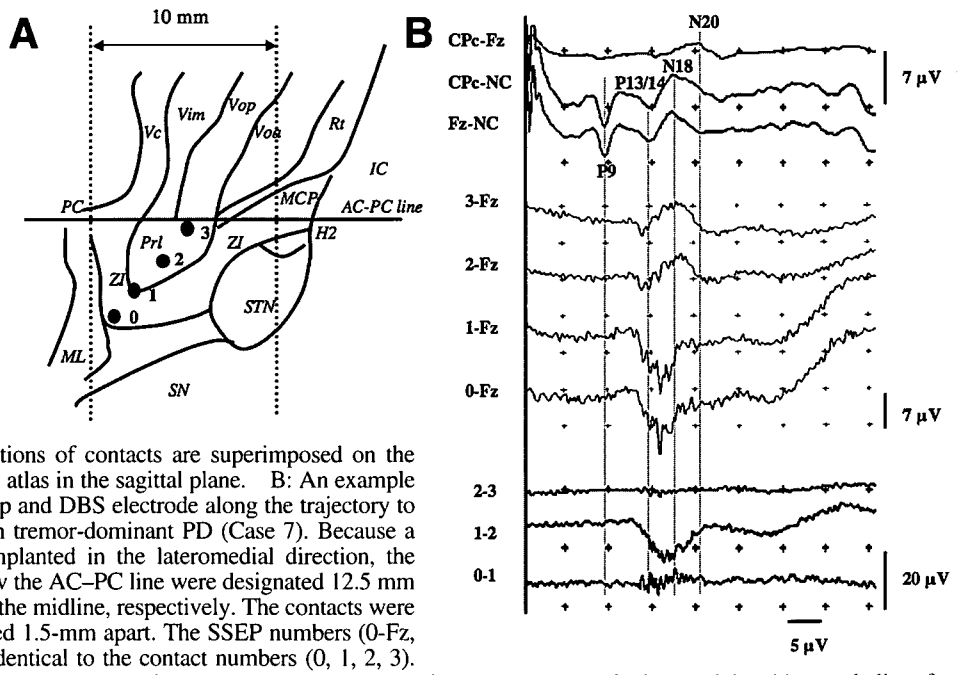

FIG. 1. A: The locations of contacts are superimposed on the Schaltenbrand–Wahren atlas in the sagittal plane. B: An example of SSEPs from the scalp and DBS electrode along the trajectory to the ZI in a patient with tremor-dominant PD (Case 7). Because a DBS electrode was implanted in the lateromedial direction, the atlases above and below the AC–PC line were designated 12.5 mm and 10.5 mm lateral to the midline, respectively. The contacts were 1.5-mm long and spaced 1.5-mm apart. The SSEP numbers (0-Fz, 1-Fz, 2-Fz, 3-Fz) are identical to the contact numbers (0, 1, 2, 3). *Dotted lines* show the latency period of P9, P13/14, N18 and N20. Somatosensory evoked potentials with a cephalic reference showed canceling of P9. The positive–negative SSEPs with a major negative polarity were recorded from the upper two contacts located in the prelemniscal radiation (2-Fz and 3-Fz). The latency of the initial positive wave was almost the same as P13/14 at the CPc-NC and Fz-NC. The latency of the major negative peak was almost the same as N18. From the lower two contacts located in the ZI, broad positive potentials with the peak latency of 16.1 msec were recorded. Many small notches were superimposed on subthalamic SSEPs, and the amplitude was the maximum at contact 0 located closest to the ML. With bipolar recordings, a broad positive potential with small notches was recorded at contact 1–2 Abbreviations: H2 = H of Forel; IC = internal capsule; MCP = mid-commissure point; Prl = prelemniscal radiation; Rt = nucleus reticularis; SN = substantia nigra; Voa = nucleus ventrooralis anterior; Vop = nucleus ventrooralis posterior. 0, 1, 2, 3 represent the contacts of the DBS electrode.

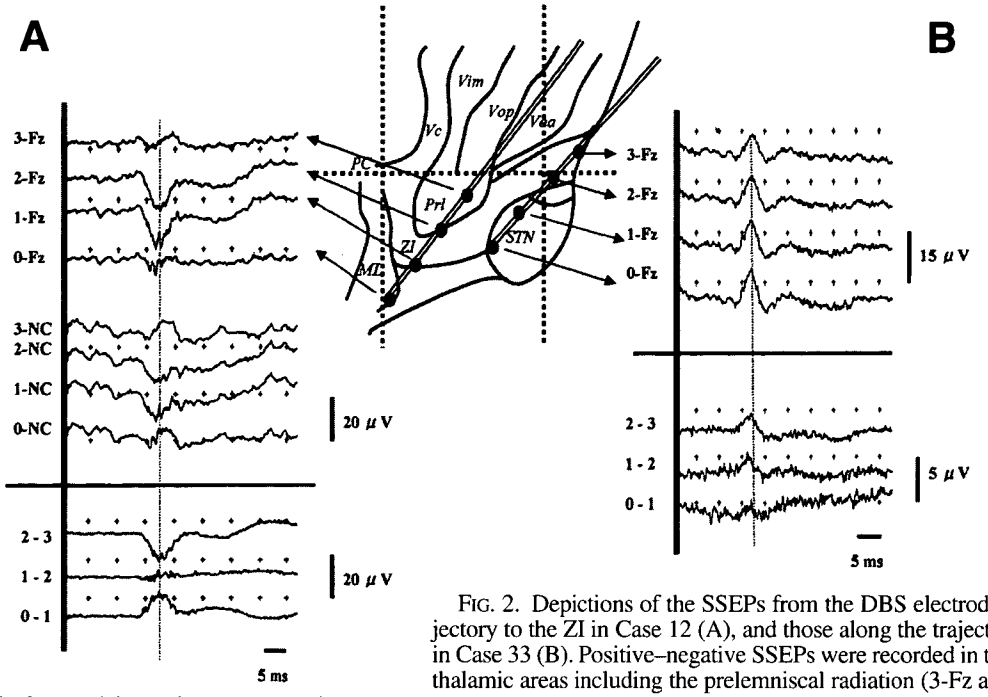

FIG. 2. Depictions of the SSEPs from the DBS electrode along the trajectory to the ZI in Case 12 (A), and those along the trajectory to the STN in Case 33 (B). Positive–negative SSEPs were recorded in the various subthalamic areas including the prelemniscal radiation (3-Fz and 3-NC in A), ML (0-Fz and 0-NC, in 2A) and STN (0-Fz and 1-Fz in B). In the ventral part of the ZI, monophasic positive potential was recorded with cephalic and noncephalic references, and with bipolar recordings (1-Fz, 2-Fz, 1-NC, 2-NC and 2–3 in A). With bipolar recordings, the potential with the same latency reversed phase between the ZI and ML (between 0–1 and 1–2 in A). In the anterior subthalamic region including the subthalamic nucleus, small negative potentials with a mean latency of 16 msec were recorded (1–2 and 2–3 in B) with bipolar recordings. These negative potentials did not show phase reversal, and amplitudes of the potentials recorded from the upper pair of contacts were larger than those recorded from the lower pair of contacts.

Monophasic Positive Wave

In the posteromedial subthalamic region, a monophasic positive wave was recorded using cephalic and noncephalic references (0-Fz and 1-Fz, Fig. 1; 1-Fz, 2-Fz, 1-NC and 2-NC, Fig. 2A). The latency of the monophasic positive wave was between P13/14 and N18 (15.8 ± 0.9 msec). The mean amplitude was 10.2 ± 4.5 μV. We designated this positive wave subthalamic P16. Subthalamic P16 was recorded only in the posteromedial subthalamic region (mean 6.6 ± 1.3 mm posterior to the MCP, 4.8 ± 1.2 mm inferior to the AC–PC line, and 9.7 ± 0.6 mm lateral to the midline, 12 SSEPs), which coincided with the ventral region of the ZI in the Schaltenbrand–Wahren atlas (*filled circles* in Fig. 3A). There was a transition of the positive–negative SSEP configurations over the boundary of the ventral region of the ZI and the immediately surrounding area (the ML and the prelemniscal radiation). Several small notches were superimposed on the monophasic positive SSEPs. Using the contact from which the monophasic positive SSEP was recorded, we applied stimulation at a low intensity, which led to improved tremor and rigidity and transient paresthesia in the contralateral hand. Using the deeper contact electrode located near the ML, we applied stimulation at 1.5 V and 130 Hz, which evoked moderate paresthesia in the entire contralateral side of the body.

Somatosensory Evoked Potentials in the Subthalamic Region With Bipolar Recordings

With bipolar recordings, we can minimize the contribution of far-field potentials. Positive potentials with a mean peak latency of 16.5 ± 1.2 msec were recorded in the ventral ZI (1-2 in Fig. 1, 2-3 in Fig. 2A, *filled circles* in Fig. 3B). The potential with reversed phase at the same latency was located immediately caudoventral to the ZI (between 0-1 and 1-2 in Fig. 2A). Negative potentials with mean a latency of 16.2 ± 0.7 msec, were recorded in the subthalamic region located immediately caudoventral to the ZI (*open triangle* in Fig. 3B).

From the pairs of contacts located in the dorsal border of the STN and the most rostral subthalamic area, small negative potentials were recorded (0-1, 1-2, and 2-3 in Fig. 2B; *filled triangles* in Fig. 3B). The mean latency was 16.0 ± 1.2 msec in 38 SSEPs. These negative potentials did not show phase reversal, and the amplitudes of the SSEPs from the lower pair of contacts were smaller than those from the upper pair of contacts (Fig. 2B). In the other subthalamic areas, no significant potentials were recorded with bipolar recordings (53% of SSEP recordings).

Discussion

We recorded SSEPs in response to contralateral median nerve stimulation from DBS electrodes implanted in subthalamic areas. Somatosensory evoked potential configurations depended on locations of the DBS electrode. Using cephalic and noncephalic references, positive–negative SSEPs at peak latencies similar to those of the scalp at P13/14 and N18 were recorded in the entire subthalamic area. In the ventral part of the ZI, a monophasic positive

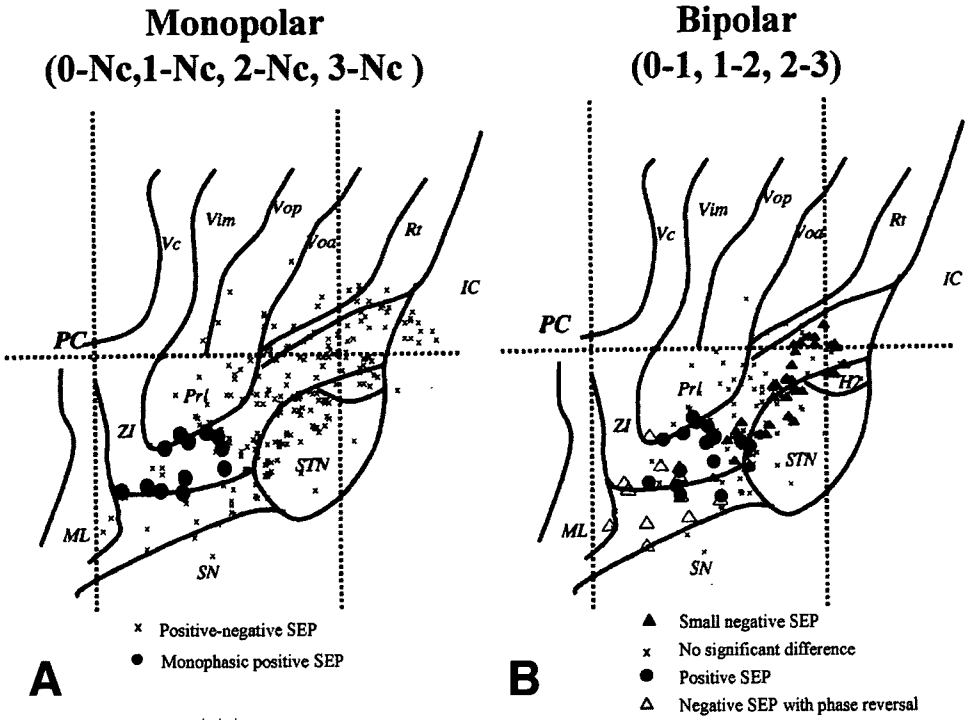

FIG. 3. The SSEPs were classified by the configuration and their distribution was mapped on the Schaltenbrand–Wahren atlas. With monopolar recordings (A), positive–negative SSEPs *(crosses)* and monophasic positive SSEPs (subthalamic P16, *filled circles*) were recorded in the subthalamic region. Subthalamic P16 was recorded in the ZI (mean 6.0 ± 1.8 mm posterior to the MCP, 4.7 ± 1.3 mm inferior to the AC–PC line, and 9.6 ± 0.6 mm lateral to the midline, 15 SSEPs). With bipolar recordings (B), subthalamic P16 *(filled circles)* was recorded from the ventromedial part of the ZI (mean 4.5 ± 1.2 mm posterior to the MCP, 3.5 ± 1.8 mm inferior to the AC–PC line, and 10.4 ± 0.9 mm lateral to the midline, 16 SSEPs). They showed phase reversal, and negative SSEPs with latency similar to that of subthalamic P16 *(open triangles)* were recorded in the subthalamic region located immediately caudoventral to the ZI. The majority of SSEPs recorded from the anterior half of the subthalamic region showed no significant potential differences *(crosses)*, but several small negative potentials *(filled triangles)*were recorded in the rostral subthalamic region including the rostral pole of the ZI, H fields of Forel and dorsal part of the STN (mean 0.1 ± 1.5 mm posterior to the MCP, 0.6 ± 2.0 mm inferior to the AC–PC line, and 12.0 ± 1.2 mm lateral to the midline).

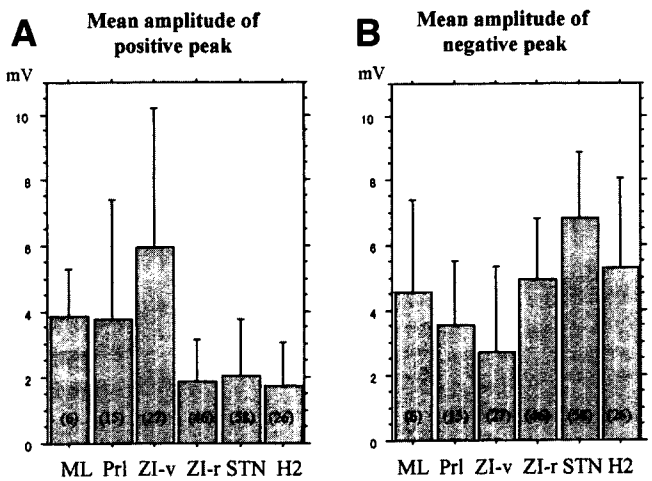

FIG. 4. Bar graphs of the mean amplitude of positive peak (A), and negative peak (B). The mean and standard error of amplitude of the positive and negative peaks with cephalic reference were calculated in relation to the recording sites. Numbers in parentheses are numbers of SSEPs. The mean amplitude of the positive peak was maximal in the ventral part of the ZI, and the maximal mean amplitude of the negative peak was in the STN, located immediately rostral to the ventral part of the ZI. Abbreviations: ZI-r = rostral part of the ZI; ZI-v = ventral part of the ZI.

SSEP at a latency of 16 msec (subthalamic P16) was recorded using both cephalic references and bipolar recordings. Because the ventral part of the ZI is a particularly effective target of DBS for severe proximal tremors,[11] subthalamic P16 can be a landmark for the assessment of the best position for DBS in the posterior subthalamic area.

Monophasic Positive Wave

Monophasic positive SSEPs at similar peak latencies to those measured at subthalamic P16 have been recorded in the Vc.[5,6,9,16] Although the amplitudes of the reported potentials were much larger than at subthalamic P16, there were many similarities between monophasic positive SSEP in the Vc and subthalamic P16. The positive SSEPs in the Vc did not extend to the immediately surrounding areas rostrally (Vim), ventrally (ML), or dorsally (the dorsal part of the Vc and the phase reversal occurred on the boundaries of the Vc–Vim and Vc–ML.[5,8] Subthalamic P16 also did not extend to the immediately surrounding areas dorsally (prelemniscal radiation), rostrally (STN), or ventrally (ML or fasciculus Q), and showed a phase reversal at the boundary of the ZI and ML. Based on these findings, we consider it

unlikely that subthalamic P16 was produced by a volume conduction of the positive potential generated at the Vc. In animal studies, the ventral subregions of the ZI have been found to receive dense direct afferent projections from the trigeminal complex and dorsal column nuclei, and to project to the sensory cortex from the rostral pole.[3,13] Somatosensory responses have been recorded in the rostral two thirds of the ZI in rats.[13] Therefore subthalamic P16 may reflect excitatory postsynaptic potentials of neurons in ZI. Because the electrophysiological features of the ZI have not been well defined in humans, more studies of neuronal activities of the human ZI are needed to prove this hypothesis. Another possibility is that subthalamic P16 represents junctional potentials from the ML. Junctional potentials are generated at the bend of the sensory tract. According to the Schaltenbrand–Wahren atlas, the ML has lateral bending at approximately 9 to 10 mm lateral to the midline. This position is compatible with the site of subthalamic P16 potential, and we cannot exclude this possibility from our present results.

Positive–Negative Wave

In previous studies, positive–negative SSEPs with major negativity have been recorded in various thalamic nuclei and in the subthalamic region including the ML, prelemniscal radiation and STN.[4–6,9,16] Because the potentials were distributed over a wide recording area and occurred at an equal latency at all recording points, the positive–negative SSEP must be a far-field potential generated by volume conduction from one certain potential generated at one site. Investigators of recent studies have suggested that the potential generated at the cuneate nucleus may partly cause the P13/14 and N18 component of the scalp and subcortical SSEPs.[5,6,9,16,17] The peak latency of the major negativity of the dorsal column SSEPs recorded from the cervicomedullary junction is identical to the scalp P13/14.[10] In the present study, most positive–negative SSEPs in the subthalamic region showed no significant potential differences in bipolar recordings, suggesting that they reflect mainly P13/14 and N18.

In bipolar recordings, small negative potentials with a peak latency of 16 msec were recorded in the rostral subthalamic area and at the dorsal border of the STN, which can be a landmark for the dorsal border of the STN. These potentials displayed a tendency for caudorostral increments in amplitudes, and did not show phase reversal. Hanajima et al.[5] also have reported similar negative potentials recorded near or in the STN at similar latencies, which also displayed a tendency toward caudorostral increments in amplitudes. These findings suggest that there is a gradient in the positive (thalamus) to negative (STN) shift that is steep at the ventral border of the thalamus. In the present study, the amplitude of the negative peak was significantly high in the STN. However, the mean peak latency of 16 msec is too short to assume the STN neurons to be a generator because the STN does not receive direct afferent nerve impulses from the medial lemniscal pathway but receives projections from neurons in the primary motor cortex.[12]

Small Notches Superimposed on Subthalamic SSEPs

Several studies have reported small notches superimposed on SSEPs in the thalamus and subthalamic region.[5,6,8,9,16] In the present study, the amplitude of the small notches superimposed on SSEPs recorded in the posterior subthalamic region was larger at the lower contact located closer to the ML, suggesting that high-frequency components of subthalamic SSEPs may be generated in the lemniscal system.

Conclusions

Our results indicate that the direct recording of SSEPs with DBS electrodes is a practical method for refining stereotactic targets in the subthalamic area. Subthalamic P16 can be a landmark for the ventral ZI. Small negative SSEPs were recorded in the rostral region of the ZI. The small negative potentials may be a landmark for the target of the electrodes for DBS of the STN.

Acknowledgment

The authors thank Mr. Tadayuki Murakami for technical assistance.

References

1. Andrade-Souza YM, Schwalb JM, Hamani C, Hoque T, Saint-Cyr J, Lozano AM: Comparison of 2-dimensional magnetic resonance imaging and 3-planar reconstruction methods for targeting the subthalamic nucleus in Parkinson disease. **Surg Neurol 63:** 357–363, 2005
2. Benabid AL, Pollak P, Gao D, Hoffmann D, Limousin P, Gay E, et al: Chronic electrical stimulation of the ventralis intermedius nucleus of the thalamus as a treatment of movement disorders. **J Neurosurg 84:**203–214, 1996
3. Berkley KJ, Budell RJ, Blomqvist A, Bull M: Output systems of the dorsal column nuclei in the cat. **Brain Res 396:**199–225, 1986
4. Hanajima R, Chen R, Ashby P, Lozano AM, Hutchison WD, Davis KD, et al: Very fast oscillations evoked by median nerve stimulation in the human thalamus and subthalamic nucleus. **J Neurophysiol 92:**3171–3182, 2004
5. Hanajima R, Dostrovsky JO, Lozano AM, Hutchison WD, Davis KD, Chen R, et al: Somatosensory evoked potentials (SEPs) recorded from deep brain stimulation (DBS) electrodes in the thalamus and subthalamic nucleus (STN). **Clin Neurophysiol 115:** 424–434, 2004
6. Katayama Y, Tsubokawa T: Somatosensory evoked potentials from the thalamic sensory relay nucleus (VPL) in humans: correlations with short latency somatosensory evoked potentials recorded at the scalp. **Electroencephalogr Clin Neurophysiol 68:**187–201, 1987
7. Kitagawa M, Murata J, Uesugi H, Kikuchi S, Saito H, Tashiro K, et al: Two-year follow-up of chronic stimulation of the posterior subthalamic white matter for tremor-dominant Parkinson's disease. **Neurosurgery 56:**281–289, 2005
8. Klostermann F, Vesper J, Curio G: Identification of target areas for deep brain stimulation in human basal ganglia substructures based on median nerve sensory evoked potential criteria. **J Neurol Neurosurg Psychiatry 74:**1031–1035, 2003
9. Morioka T, Shima F, Kato M, Fukui M: Origin and distribution of thalamic somatosensory evoked potentials in humans. **Electroencephalogr Clin Neurophysiol 74:**186–193, 1989
10. Morioka T, Tobimatsu S, Fujii K, Fukui M, Kato M, Matsubara T: Origin and distribution of brain-stem somatosensory evoked potentials in humans. **Electroencephalogr Clin Neurophysiol 80:** 221–227, 1991
11. Murata J, Kitagawa M, Uesugi H, Saito H, Iwasaki Y, Kikuchi S, et al: Electrical stimulation of the posterior subthalamic area for the treatment of intractable proximal tremor. **J Neurosurg 99:** 708–715, 2003
12. Nambu A, Takada M, Inase M, Tokuno H: Dual somatotopical

representations in the primate subthalamic nucleus: evidence for ordered but reversed body-map transformations from the primary motor cortex and the supplementary motor area. **J Neurosci 16:** 2671–2683, 1996
13. Nicolelis MA, Chapin JK, Lin RC: Somatotopic maps within the zona incerta relay parallel GABAergic somatosensory pathways to the neocortex, superior colliculus, and brainstem. **Brain Res 577:**134–141, 1992
14. Plaha P, Ben-Shlomo Y, Patel NK, Gill SS: Stimulation of the caudal zona incerta is superior to stimulation of the subthalamic nucleus in improving contralateral parkinsonism. **Brain 129:** 1732–1747, 2006
15. Saint-Cyr JA, Hoque T, Pereira LC, Dostrovsky JO, Hutchison WD, Mikulis DJ, et al: Localization of clinically effective stimulating electrodes n the human subthalamic nucleus on magnetic resonance imaging. **J Neurosurg 97:**1152–1166, 2002
16. Shima F, Morioka T, Tobimatsu S, Kavaklis O, Kato M, Fukui M: Localization of stereotactic targets by microrecordings of thalamic somatosensory evoked potentials. **Neurosurgery 28:**223–230, 1991
17. Sonoo M, Genba K, Zai W, Iwata M, Mannen T, Kanazawa I: Origin of the widespread N18 in median nerve SEP. **Electroencephalogr Clin Neurophysiol 84:**418–425, 1992
18. Velasco F, Jimenez F, Perez ML, Carrillo-Ruiz JD, Velasco AL, Ceballos J, et al: Electrical stimulation of the prelemniscal radiation in the treatment of Parkinson's disease: an old target revised with new techniques. **Neurosurgery 49:**293–308, 2001
19. Voges J, Volkmann J, Allert N, Lehrke R, Koulousakis A, Freund HJ, et al: Bilateral high-frequency stimulation in the subthalamic nucleus for the treatment of Parkinson disease: correlation of therapeutic effect with anatomical electrode position. **J Neurosurg 96:**269–279, 2002

Manuscript submitted December 14, 2006.
Accepted February 13, 2007.
Address reprint requests to: Mayumi Kitagawa, M.D., Ph.D., Sapporo Azabu Neurosurgical Hospital, North-40 East-1, Higashi-ku, Sapporo 007–0840, Japan. email: kitagawa-jscn@umin.ac.jp.

Bioelectromagnetics 28:553–561 (2007)

Effects of High Frequency Electromagnetic Field (EMF) Emitted by Mobile Phones on the Human Motor Cortex

Satomi Inomata-Terada, Shingo Okabe, Noritoshi Arai, Ritsuko Hanajima, Yasuo Terao, Toshiaki Frubayashi, and Yoshikazu Ugawa*

Department of Neurology, Graduate School of Medicine, the University of Tokyo, Tokyo, Japan

We investigated whether the pulsed high frequency electromagnetic field (EMF) emitted by a mobile phone has short term effects on the human motor cortex. We measured motor evoked potentials (MEPs) elicited by single pulse transcranial magnetic stimulation (TMS), before and after mobile phone exposure (active and sham) in 10 normal volunteers. Three sites were stimulated (motor cortex (CTX), brainstem (BST) and spinal nerve (Sp)). The short interval intracortical inhibition (SICI) of the motor cortex reflecting GABAergic interneuronal function was also studied by paired pulse TMS method. MEPs to single pulse TMS were also recorded in two patients with multiple sclerosis showing temperature dependent neurological symptoms (hot bath effect). Neither MEPs to single pulse TMS nor the SICI was affected by 30 min of EMF exposure from mobile phones or sham exposure. In two MS patients, mobile phone exposure had no effect on any parameters of MEPs even though conduction block occurred at the corticospinal tracts after taking a bath. As far as available methods are concerned, we did not detect any short-term effects of 30 min mobile phone exposure on the human motor cortical output neurons or interneurons even though we can not exclude the possibility that we failed to detect some mild effects due to a small sample size in the present study. This is the first study of MEPs after electromagnetic exposure from a mobile phone in neurological patients. Bioelectromagnetics 28:553–561, 2007.

Key words: mobile phone; transcranial magnetic stimulation (TMS); hot bath effect; motor evoked potential (MEP); multiple sclerosis; conduction block

INTRODUCTION

Widespread use of mobile phones has given rise to a growing concern for their possible adverse effects on the human central nervous system. Mobile phones emit pulsed high frequency electromagnetic field (EMF) may have some effects on the brain. Many studies have investigated the effects of mobile phones on the human brain function [Reiser et al., 1995; Eulitz et al., 1998; Freude et al., 1998; Urban et al., 1998; Borbely et al., 1999; Hladky et al., 1999; Kellényi et al., 1999; Preece et al., 1999; Huber et al., 2000, 2002; Koivisto et al., 2000; Krause et al., 2000, 2004; Sandstrom et al., 2001; Croft et al., 2002; Ozturan et al., 2002; Arai et al., 2003; Bak et al., 2003; Lee et al., 2003; Hamblin et al., 2004; Maby et al., 2005], some of which showed non-thermal bioeffects of mobile phones [Reiser et al., 1995; Borbely et al., 1999; Kellényi et al., 1999; Huber et al., 2000; Hamblin et al., 2004; Maby et al., 2005]. Some of the studies used evoked potentials [Urban et al., 1998; Kellényi et al., 1999; Arai et al., 2003; Bak et al., 2003; Hamblin et al., 2004; Maby et al., 2005], one kind of objective analysis of human brain function, during and after mobile phone exposure. On the other hand, one review article stressed the importance of secondary, indirect effects rather than direct biological effects of mobile phone exposure [Hossmann and Hermann, 2003]. Sandstrom et al. [2001] reviewed many papers on the effects of the mobile phone and cautioned that we should not conclude that any

Grant sponsor: The Committee to Promote Research on the Possible Biological Effects of Electromagnetic Fields, the Ministry of Internal Affairs and Communications (MIC), Japan. Research Project Grant-in-aid for Scientific Research from the Ministry of Education, Culture, Sports, Science and Technology of Japan; Grant number: 16500194.

*Correspondence to: Dr. Yoshikazu Ugawa, Department of Neurology, Division of Neuroscience, Graduate School of Medicine, University of Tokyo, 7-3-1, Hongo, Bunkyo-ku, Tokyo 113-8655, Japan. E-mail: ugawa-tky@umin.net

Received for review 6 February 2006; Final revision received 1 January 2007

DOI 10.1002/bem.20318
Published online 21 May 2007 in Wiley InterScience (www.interscience.wiley.com).

evoked effects are produced by pulsed EMF before excluding various other physical factors associated with using a mobile phone. Exclusion of such confounding factors warrants control experiments using appropriate sham exposures. In this paper, therefore, we compared the results between real and sham exposures.

Previously we have shown that no short term adverse effects were elicited by 30 min of mobile phone exposure on auditory brainstem responses (ABRs), middle latency responses (MLRs) [Arai et al., 2003] or somatosensory evoked potentials (SEPs) [Yuasa et al., 2006]. Other groups have employed visual evoked potentials (VEPs) to investigate possible bioeffects of mobile phone exposure [Urban et al., 1998; Hladky et al., 1999] and showed no significant effects. The reaction times were not affected by the mobile phone exposure [Hamblin et al., 2006; Terada et al., 2006]. Even though TMS is very useful in investigating motor cortex physiology in humans, there have been no reports of effects of mobile phones on the human motor cortex using transcranial magnetic stimulation (TMS). In this article, comparing motor evoked potentials (MEPs) before and after mobile phone exposure, we have studied short term effects of pulsed EMF from a mobile phone on the motor cortex in normal human subjects. To investigate the possible effects of pulsed EMF on the GABAergic inhibitory interneuronal function of the motor cortex [Ziemann et al., 1996a], we studied the short interval intracortical inhibition (SICI) using paired pulse TMS [Kujirai et al., 1993].

Because many neurological patients may use a mobile phone as usual people do, we should investigate whether it affects some parts of the brain in patients, especially in those who have some temperature dependent neurological symptoms. We had the chance to observe two patients with multiple sclerosis showing conduction block in the corticospinal tracts after taking a bath (hot bath effect). This indicated that their corticospinal tracts were more susceptible to high temperature than those of normal subjects. Therefore, we studied the effects of mobile phone exposure on the central motor pathways in these patients to see whether such susceptible tracts are particularly vulnerable to the effect of EMF emitted by a mobile phone. Additionally, we would inquire whether mobile phone exposure causes an increase in core temperature similar to that caused by taking a hot bath.

As we would expect the mobile phone induced effects to be greatest during exposure, we were interested in possible changes in the motor cortex when the EMF was given. However, as we could not perform TMS during exposure due to the possible interference of the mobile phone-emitted EMF, we compared MEPs before and after exposure.

SUBJECTS AND METHODS

Ten normal volunteers (5 men and 5 women, age 22 to 51 years) participated in this investigation. Although the sample size of 10 or less may not be sufficient enough to detect a very mild effect from a mobile phone, many papers have shown some mild, unnoticed effects on the motor cortex in ten subjects or less. For example, in smaller number of subjects, mild effects on the motor cortex were detected by TMS, especially by paired pulse TMS in the case of drug intake [Ziemann et al., 1996b; Ziemann, 2004], motor imagery [Kasai et al., 1997] and so on. Therefore, in the present article, we studied ten normal subjects. We also studied two patients with multiple sclerosis (MS) who had weakness after taking a bath (hot bath effect). Although the number of two was again not sufficient for statistical comparison, I have examined only four MS patients (including the present two patients) showing paralysis after taking a bath in my 25-year clinical career. Therefore, we studied the two MS patients in the present article. The subjects all gave their written informed consent to participate in the study, which was approved by the ethics committee of the University of Tokyo according to the Declaration of Helsinki.

Single pulse TMS experiments were done before and after EMF exposure in all 10 normal subjects and two patients. In normal subjects, the same experiments were repeated before and after sham exposure. In the two patients, we performed the same experiments again before and after taking a bath to confirm a so-called hot bath effect. In ten normal subjects, paired pulse TMS experiments were also performed to study the SICI of the motor cortex reflecting its GABAergic function.

Pulsed EMF was given with a handset (Matsushita communication P97-7051-0) connected to a cellular phone simulator (Digital cellular phone communication tester, NJR-920). It was set to emit its maximum output comparable to the maximum output of usual Japanese mobile phones. In order to investigate whether the mobile phone had an effect on the brain when the maximum output was continuously given, we set it at the maximum output. The mobile phone employed for the current experiments transmitted in the 800 MHz frequency band, used aπ/4 shifted Quadrature Phase-Shift Keying (QPSK) modulation shame; multiple access; three channel time division multiple access (TDMA); 20 ms, time slot; 6.7 ms, maximum transmitting power; 270 mW as the averaged value (0.8 W of burst power). The handset was oriented in normal position for use over the left ear and the microphone oriented towards the corner of the mouth. The top of the antenna was located about 4 cm from the head. The subject held the handset for 30 min in a position

similar to normal use. Because they could not fix it at exactly the same position for 30 min, specific absorption rate (SAR) in the brain was not mathematically constant throughout the experiment. However, we asked the subjects to keep the position of the handset as still as possible for 30 min. We used this exposure because we considered it appropriate for studying effects of mobile phone exposure on the brain during use in daily life. SARs at the brain area (3 cm below the skull under the coil) were measured using a phantom system for SAR measurement recommended by the IEC (International Electrotechnical Commission) standard [IEC, 2003]. This measurement was performed at several conditions in which the handset was fixed at different positions to the phantom similarly seen when we hold a handset in daily life. They were within $.054 \pm .02$ W/kg of 10 g averaged value in our experiments. These values did not differ between several positions of the handset. In the sham exposure, the experimental setting was the same as the real exposure except that the EMF was turned off. Just before and after the real or sham exposure, we performed single and paired pulse TMS experiments. The exposure condition was blinded to the subjects and experimenters performing TMS experiments.

In two patients with MS, we recorded MEPs before and after taking a bath for 30 min. A period of 30 min was long enough to induce reversible mild weakness (hot bath effect). The temperature of hot water was set at 42 °C.

Single Pulse TMS Experiment

Subjects sat comfortably on a reclining chair with their arms supported. Surface electromyographic (EMG) activities were recorded from the right first dorsal interosseous muscle (FDI) with a pair of surface cup electrodes in a belly-tendon montage. Signals were amplified with filters set at 100 Hz and 3 KHz and recorded at sampling rate of 10000 Hz by a computer (Signal Processor DP-1200, GE Marquette Medical Systems) for later off-line analysis.

TMS was performed according to the previously described methods [Ugawa et al., 1994]. TMS was delivered with a figure-of-eight-shaped coil (outer diameter of each wing was 7 cm) connected to a Magstim 200 magnetic stimulator (The Magstim Co., Ltd., Whitland, UK). For motor cortical stimulation, the coil was positioned over the hand area of the left primary motor cortex (M1) (the motor cortex innervating the target muscle). In our experiments, M1 was defined as the position where stimulation evoked the largest MEP from the right first dorsal interosseous (FDI) muscle. In two normal subjects, that position was confirmed to lie over the primary motor cortex by the neuronavigation system. The coil was oriented to induce currents antero-medially in the brain, which is perpendicular to the central sulcus. For brainstem stimulation, we used a double cone coil, the center of which was placed over 2–3 cm below the inion on the median line. The coil currents were set to induce upward currents in the brain [Ugawa et al., 1994]. For cervical motor root stimulation, we placed a round coil with its upper edge positioned over the spinous process of the seventh cervical vertebra. For cortical or brainstem stimulation, the subjects maintained a weak constant voluntary contraction of the FDI; for cervical stimulation, they relaxed it. In each stimulation condition, the intensity was increased to evoke supramaximal MEPs in normal subjects or up to the maximal stimulator output in the two patients. In each stimulation condition, TMS was repeated at least twice to assess the reproducibility of the findings.

We measured the size and onset latency of all MEPs to motor cortical, brainstem and cervical stimulation and compared them before and after mobile phone exposure, sham exposure or taking a bath. For normal subjects, we compared all measured parameters (latency and amplitude) among the four conditions (before and after real or sham exposure) using paired Student's t-test with compensation for multiple comparisons (Bonferroni correction). Statistical significant level after compensation was set at $P < .05$ (before compensation $P < .0125$). For each of the two patients, instead of group comparison between normal subjects and the patients, we judged whether some changes occurred after a hot bath or mobile phone exposure according to the following criteria. Because the sample size of two was not sufficient for statistical comparison and measured values varied due to variable positions of lesions in patients, their results were not fit to statistical comparisons between the groups. Therefore, we evaluated significant changes in each patient individually. When the MEP latency was shortened or prolonged by more than .7 ms or its amplitude changed in the amount of more than 32 % of the control MEP, we judged them as significant changes. These criteria were based on our clinical experiences that in the same muscle of normal subjects, the mean ($\pm$SD) latency variability was $.3 \pm .2$ ms and amplitude variability was $20 \pm 6\%$ of MEP amplitude. Their mean + 2 SDs were .7 ms and 32%.

Paired Pulse TMS Experiment to Study the SICI of the Motor Cortex

We studied the short interval intracortical inhibition [Kujirai et al., 1993; Hanajima et al., 1996] of the motor cortex in all normal subjects. Conditioning and

test stimuli were given through the same figure-eight shaped coil by connecting two magnetic stimulators linked with a Bistim module.

We first determined the threshold using averaged rectified EMGs for active muscles (average of at least 10 responses). The intensity of stimulation was changed in steps of 2% of the maximum stimulator output. We defined the active threshold as the lowest intensity that evoked a small response (about 50 μV) compared to the pre-stimulus background activities in averaged responses. The intensity of the conditioning stimulus was set at −2% of the maximum output below this threshold. The test stimulus was adjusted to evoke a response approximately .5 mV peak to peak in the active FDI, which was 10 to 15% above the threshold. We used a randomized conditioning-test design similar to that reported previously [Hanajima et al., 1996]. In short, various conditions (a test or conditioning stimulus given alone, and a test stimulus preceded by a conditioning stimulus at various ISIs) were intermixed randomly in one block. A few blocks of trials were performed to investigate the entire time course of the studied effect. Interstimulus intervals (ISIs) between 1 and 5 ms (1, 2, 3, 4, and 5 ms) were used. Eight to 10 responses were collected and averaged for each condition in which both stimuli were given and 20 responses for a control condition in which the test stimulus was given alone. The peak-to-peak amplitude of single responses under each condition was measured to statistically compare the amplitudes of control and conditioned responses in the same block with a t-test corrected for multiple comparisons (Bonferroni correction) in each single subject. We calculated the ratio of the mean amplitude of the conditioned response to that of the control response for each ISI in every subject. The graphs plot the mean (± standard error: SE) time course of the effect of the conditioning stimulus with the mean ratios from all normal subjects against the ISI.

We compared time courses for the four conditions using repeated measures ANOVA. The dependent variables were the size ratios of MEP amplitudes. The timing of two levels (before and after exposure), mode of exposure of two levels (real and sham exposure) and the interval of five levels (1, 2, 3, 4, and 5 ms) were independent factors. The interval was a repeated factor. The Greenhouse–Geisser correction was used to correct for nonsphericity. When an ANOVA test showed significant effects, we further performed post-hoc analyses with Student's *t*-test with compensation for multiple comparisons (Bonferroni correction). The statistical tests were performed with SPSS 10 software, and the significance level was set at 5%.

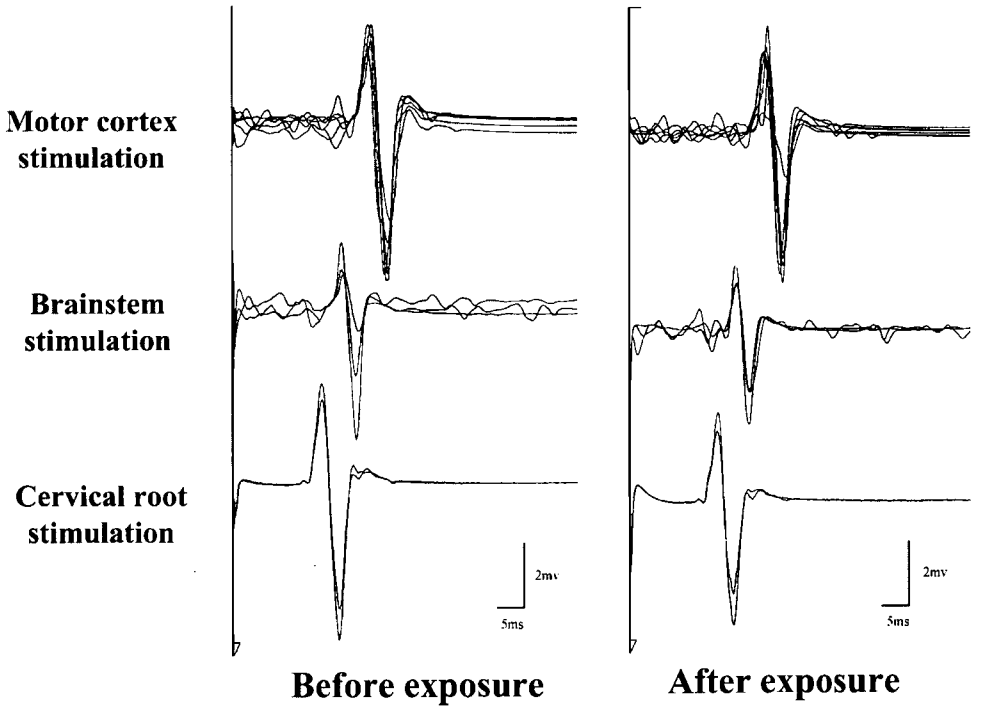

Fig. 1. MEPs before and after EMF exposure from a mobile phone in a normal subject. Several single MEPs from the first dorsal interosseous muscle are superimposed in each trace. MEPs before exposure are shown on the left and those after on the right. Top traces are cortical MEPs, middle traces MEPs to brainstem stimulation, and bottom traces MEPs to cervical stimulation. No changes were seen in any responses before and after the exposure.

RESULTS

Pulsed EMF Effects on the Central Motor Pathways in Normal Subjects

Figure 1 shows one example of MEPs before and after 30 min of EMF exposure in a single normal subject. In all MEPs to motor cortical, brainstem and cervical stimulation, their latencies and amplitudes after the EMF exposure were not different from those before. Table 1 shows mean (± SD) latencies and amplitudes of MEPs to single pulse TMS. There were no significant differences between the 4 conditions for any parameters (paired Student's t-test with Bonferroni correction; $P > .10$). This suggested that

TABLE 1. Mean ± SD of Parameters of MEP Before and After EMF Exposure and Sham Exposure

	Real exposure		Sham exposure	
	Before	After	Before	After
Latency (ms)				
Cortical	19.2 ± 1.5	19.3 ± 1.6	19.4 ± 1.5	19.2 ± 1.5
Brainstem	16.6 ± 0.8	16.5 ± 1.0	16.7 ± 0.6	16.6 ± 0.8
Cervical	13.0 ± 0.7	13.2 ± 1.0	13.1 ± 0.8	13.0 ± 0.9
Amplitude (μV)				
Cortical	3.9 ± 2.7	4.1 ± 3.0	3.8 ± 2.3	4.0 ± 2.5
Brainstem	2.0 ± 2.3	1.9 ± 2.1	2.1 ± 1.6	2.0 ± 1.6
Cervical	3.9 ± 3.4	3.6 ± 3.1	3.8 ± 2.5	3.7 ± 2.6

None of the parameters differed significantly between before and after or between real and sham exposure.

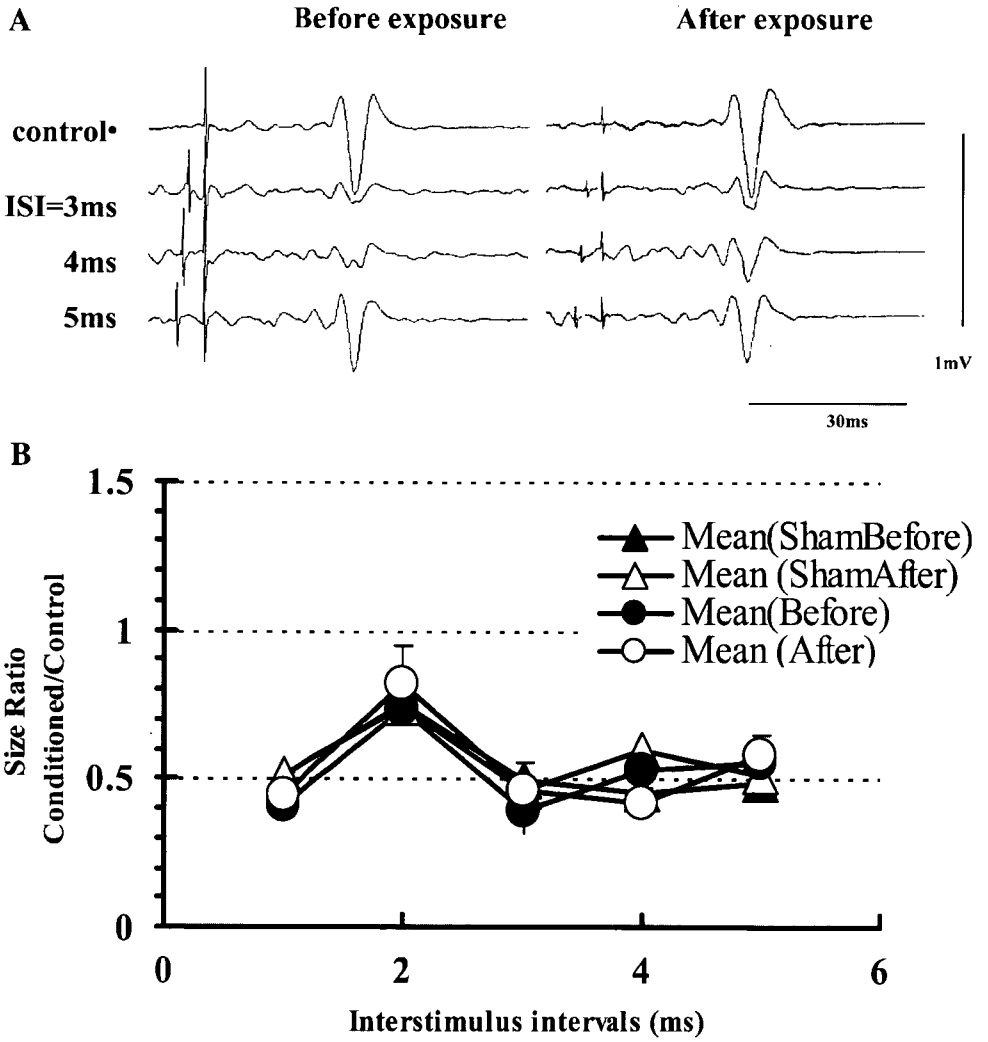

Fig. 2. **A**: Cortical MEPs of the paired pulse TMS experiment in a normal subject. MEPs before exposure are shown on the left side and those after on the right. Top traces are average control MEPs, the other traces are average conditioned MEPs at ISIs of 3, 4, 5 ms. All conditioned MEPs were smaller than the control MEPs. **B**: Average time courses for short interval intracortical inhibition before and after 30 min of EMF exposure and sham exposure. The inhibition was seen at all studied interstimulus intervals in all four conditions. ANOVA revealed no significant effects of the timing (before and after the exposure) or the mode of exposure (real and sham exposure) on the time course.

neither thirty minutes of EMF exposure nor sham exposure had any effect on MEPs to single pulse TMS in normal subjects.

Paired Pulse TMS in Normal Subjects

Figure 2A shows MEPs of the paired pulse TMS experiment in one normal subject. Suppression was noted at ISIs of 3, 4, and 5 ms both before and after exposure. In all normal subjects, significant suppression was evoked at all ISIs from 1 to 5 ms under all four conditions (before and after the real or sham exposure). We compared the time courses of suppression between the four conditions. Mean time courses for the four conditions are shown in Figure 2B. Statistical comparisons of SICI are summarized in Table 2. ANOVA revealed a significant effect of ISI, whereas neither the timing (before or after the exposure) nor the mode of exposure (sham or real exposure) had significant effects. There were no significant interactions between the interval and timing, timing and mode or between interval and mode of exposure, nor was there a significant interaction among three factors (ISI, timing, mode of exposure). The size ratio at 2 ms was slightly greater than those at the other ISIs, which is consistent with our previous report [Hanajima et al., 2003]. These results suggest that the SICI did not differ significantly before and after the real or sham exposure. Thus, neither real nor sham exposure had significant effects on the SICI of the motor cortex.

Central Motor Conduction in Two Patients with MS

A 45-year-old man with MS often had left hemiparesis after taking a bath which disappeared by cooling about 1 h after the bath. He had had MS for 12 years. Magnetic resonance images (MRIs) of the brain disclosed an active plaque at the base of the right midbrain involving cerebral peduncle. Figure 3A shows MEPs to single pulse TMS before and after taking a bath. Similar sized MEPs were elicited at almost the same latency in brainstem and cervical stimulation before and after the bath. Before taking a bath, the brainstem latency was 18.3 ms and cervical latency was 13.8 ms. Both of them were within the normal range. However, the cortical latency of 25.8 ms was abnormally prolonged. These results suggested that a lesion affected the corticospinal tracts between the motor cortex and foremen magnum, which was compatible with a lesion shown by MRI at the cerebral peduncle. The latencies after taking a bath were 25.9, 18.5, and 13.9 ms, respectively, each of which did not differ from those before the bath. In contrast to latencies, the amplitudes showed some changes after a bath. In spite of an absence of changes in amplitude in brainstem and cervical stimulation, MEPs to cortical stimulation were smaller after the bath than before it. This indicated that, after taking a bath, conduction block occurred in the corticospinal tracts at some intracranial level, probably at the cerebral peduncle. Figure 3B shows MEPs before and after the pulsed EMF exposure in the same patient. Neither latencies nor amplitudes were affected by 30 min of mobile phone exposure. MEPs to motor cortical stimulation were almost the same in size before and after the EMF exposure although their sizes were suppressed after a bath.

In another MS patient having a hot bath effect, the EMF exposure emitted by mobile phones did not affect any parameters of MEPs to three kinds of stimulation even though cortical MEP amplitudes decreased after a bath.

These results suggested that mobile phone exposure had no effect on the corticospinal tract lesions susceptible to high body temperature.

TABLE 2. Analysis of Variance Test for the Short Interval Intracortical Inhibition of the Motor Cortex

Short interval intracortical inhibition (SICI)				
	DF1	DF2	*F*-value	*P*-value
ISI	2.293	32.096	8.146	.01*
Mode of stimulation (Mode)	1	14	.094	.763
Before and after the phone use (B/A)	1	14	.444	.516
ISI × mode	2.293	32.096	.51	.630
ISI × B/A	2.311	32.635	.046	.97
Mode × B/A	1	14	.09	.926
ISI × mode × B/A	2.311	32.635	3.081	.073

DF, degree of freedom; ISI, interstimulus interval.
*statistically significant.

DISCUSSION

Before the main discussion, it should be noted that our normal values for MEP amplitude were smaller than those reported previously, whereas the normal values for MEP latency were consistent with others. This is explained by the difference in EMG recording, that is, the low cut filter in our recording was set at a relatively high value (100 Hz). EMG responses recorded with a low cut filter of 100 Hz are half to two-thirds the size of those recorded with 10 Hz low cut filter. Therefore, our normal values of amplitude were actually consistent with those of other previous articles [De Rosa et al., 2006].

In normal subjects, no effects were detected on either the corticospinal tract neurons or interneurons of the motor cortex in the pulsed EMF exposure from

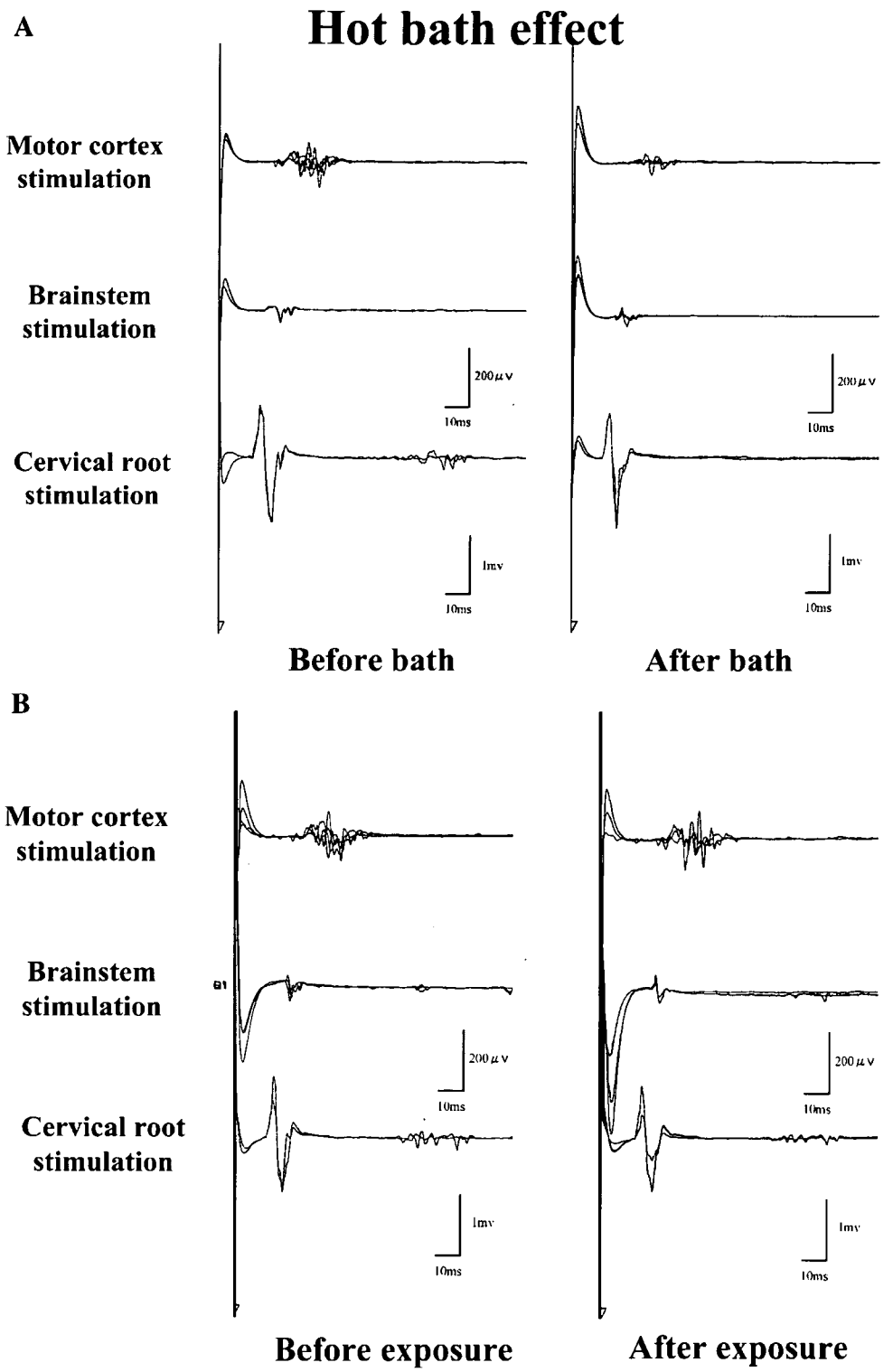

Fig. 3. **A**: MEPs before (**left**) and after (**right**) taking a bath in a patient with multiple sclerosis. A few single MEPs are superimposed. Cortical MEPs are shown at the top row, those to brainstem stimulation at the middle, and MEPs to cervical stimulation at the bottom. The sweep time was twice as long as that of Figure 1. Cortical MEPs were smaller after taking a bath than those before, even though responses to brainstem or cervical stimulation showed no changes. This suggests that taking a bath evoked conduction block in the corticospinal tracts between the cortex and brainstem. **B**: MEPs before and after the mobile phone exposure in the patient shown in (B). MEPs are shown in the same pattern as (A). MEPs were not affected by the EMF exposure.